Binding of CYP2C9 with Diverse Drugs and its Implications for Metabolic Mechanism

Jing-Fang Wang[1,§], Jing-Yi Yan[2,§], Dong-Qing Wei[2,3,*] and Kuo-Chen Chou[3]

[1]*Bioinformatics Center, Key Lab of Systems Biology, Shanghai Institutes for Biological Sciences, Chinese Academy of Sciences, Shanghai 200031, China;* [2]*College of Life Science and Biotechnology, Shanghai Jiaotong University, Shanghai 200240, China;* [3]*Gordon Life Sciences Institute, 13784 Torrey Del Mar Drive, San Diego, California 92130, USA*

Abstract: Cytochrome P450 2C9 (CYP2C9) is an important member of the cytochrome P450 enzyme superfamily with responsibility for metabolizing many important exogenous and endogenous compounds in many species of microorganisms, plants and animals. CYP2C9 is related to the oxidative of 16% of all therapeutics in current clinical use and has adverse drug effects, such as, enzyme induction and inhibition. In order to understand the metabolic mechanism of various drugs, two crystal structures of CYP2C9 have been studied, and their structural differences and structure-activity relationships with the drugs of Fluoxetine, Ibuprofen, Naproxen, Suprofen, and Mefenamic acid were investigated. By a series of docking studies and MD simulations, the binding pockets of CYP2C9 for the five drugs are explicitly defined that will be very useful for conducting mutagenesis studies, providing insights into the metabolic mechanism, which may be of relevance to the personalized drug.

Key Words: CYP2C9, cytochrome P-450, structure-activity relationship, metabolic mechanism.

[#]**Author Profile:** Dr. Kuo-Chen Chou is the chief scientist of Gordon Life Science Institute. He is also an Advisory Professor of several Universities. Professor Chou has published over 350 papers in the fields of computer-aided drug design, bioinformatics, protein-structural prediction, low-frequency internal motion of protein and DNA and its biological functions, graphic rules in enzyme kinetics and other biological systems, and diffusion-controlled reactions of enzymes. For more information about Professor Kuo-Chen Chou, visit http://gordonlifescience.org/members/kcchou/ or http://home.roadrunner.com/~kchou/contacts.html, or http://www.pami.sjtu.edu.cn/people/kcchou/.

INTRODUCTION

Cytochrome P450 proteins are membrane-associated haem proteins that metabolize important exogenous and endogenous compounds in many species of microorganisms, plants and animals [1]. Also, they are considered as one of the most important enzymes in the phase I metabolism in mammals [2]. Mammalian CYP450s recognize and metabolize diverse xenobiotics such as drugs, environmental compounds, retinoids and steroids [3]. This kind of enzymes can be found in all kingdoms of life and show the extraordinary diversity in their reaction chemistry. In mammals, as well as many other cell types, they are found mainly in the membranes of the endoplasmic reticulum (microsomes) within liver cells (hepatocytes), and are capable of utilizing haem iron to oxidize molecules, and often making them more water-soluble for clearance by either adding or unmasking a polar group [4]. Polymorphic variants have already been reported for some CYP450 isoforms, which has relation for the efficacy of drugs in individuals, and for the co-administration of drugs. Individual CYPs exhibit unique substrate specificity, regio- and stereoselectivity, especially CYP2C9.

*Address correspondence to this author at the College of Life Science and Biotechnology, Shanghai Jiaotong University, Shanghai 200240, China; E-mail: dqwei@gordonlifescience.org

People can carry different alleles of CYP genes, which have a little variation in their genetic sequence attributable to nucleotide changes or polymorphisms [5]. These polymorphic variations are capable of causing individual and population differences in the tolerance to toxins and drugs. Because CYP proteins are activated, polymorphic variations in different CYP genes may have different effects [6]. CYP2C9 is among the most important drug metabolizing isoforms [7]. It controls the oxidative metabolism of 16% of all therapeutics in current clinical use and it has adverse drug effects, for example, enzyme induction and inhibition.

Computational and mathematical approaches, such as structural bioinformatics [8,9], molecular docking [10-15], molecular packing [16,17], pharmacophore modelling [18, 19], Mote Carlo simulated annealing approach [20], graph and image analysis [21-33], study of low-frequency internal motions in proteins and DNA [34-36], QSAR [37-42], protein subcellular location prediction [43-48], identification of membrane proteins and their types [49], identification of enzymes and their functional classes [50], identification of GPCR and their types [51,52], identification of proteases and their types [53,54], protein cleavage site prediction [55-57], and signal peptide prediction [58,59], can timely provide very useful information and insights for biomedicine and drug development. The present study was initiated in an at-

1573-4064/09 $55.00+.00

tempt to use molecular docking and molecular dynamics to perform a detailed structural analysis to further stimulate the personalized drug design studies [12,60-63].

In the current study, CYP2C9 was picked up as a main target. In the Protein Data Bank (PDB), there are two crystal structures of CYP2C9, namely 1OG5 and 1R9O, respectively. The objective of the current study was to perform a detailed examination of the structural differences between the two different crystal structures of CYP2C9. By all-round analysis, some structural differences of the two crystal structures have been discussed. Subsequently, several drugs metabolized by CYP2C9 have been docked to the two crystal structures. Finally, the docking results are optimized by molecular dynamics simulations [64], with the purpose of analyzing the interactions between CYP2C9 and the drugs metabolized by CYP2C9, and further revealing the possible mechanism of drug metabolism presided over by cytochrome P450s.

METHOD

Computational docking operation is a useful vehicle for investigating the interaction of a protein receptor with its ligand and revealing their binding mechanism as demonstrated by a series of studies [8,10,11,13-15,19,60,65-77]. In the current study, the AutoDock 3 was used to perform all the protein-ligand docking experiments [78]. During our simulations, the proteins were kept rigid with ligand being allowed to move freely. Some solvent parameters were incorporated during the docking operation to simulate all the surrounding liquid particles explicitly. The chemical affinity and electrostatics maps were computed and centered by autogrid on receptor with 40×40×40 grid points at spacing of 0.375Å at the active sites of the two crystal structures. In addition, Lamarckian Genetic algorithm was used to search the most favorable conformations. The docking operations were carried out with 100 GA runs and 50 populations. The maximum number of energy evaluations and maximum number of generations are 250000000 and 1000, respectively. The maximum number of top individuals that automatically survive is 1. While the rate of gene mutation and rate of crossover are 0.02 and 0.8, respectively. The mean of Cauchy distribution for gene mutation and variance of Cauchy distribution for gene mutation are 0.0 and 1.0, respectively. The number of generations for picking worst individual is 10.

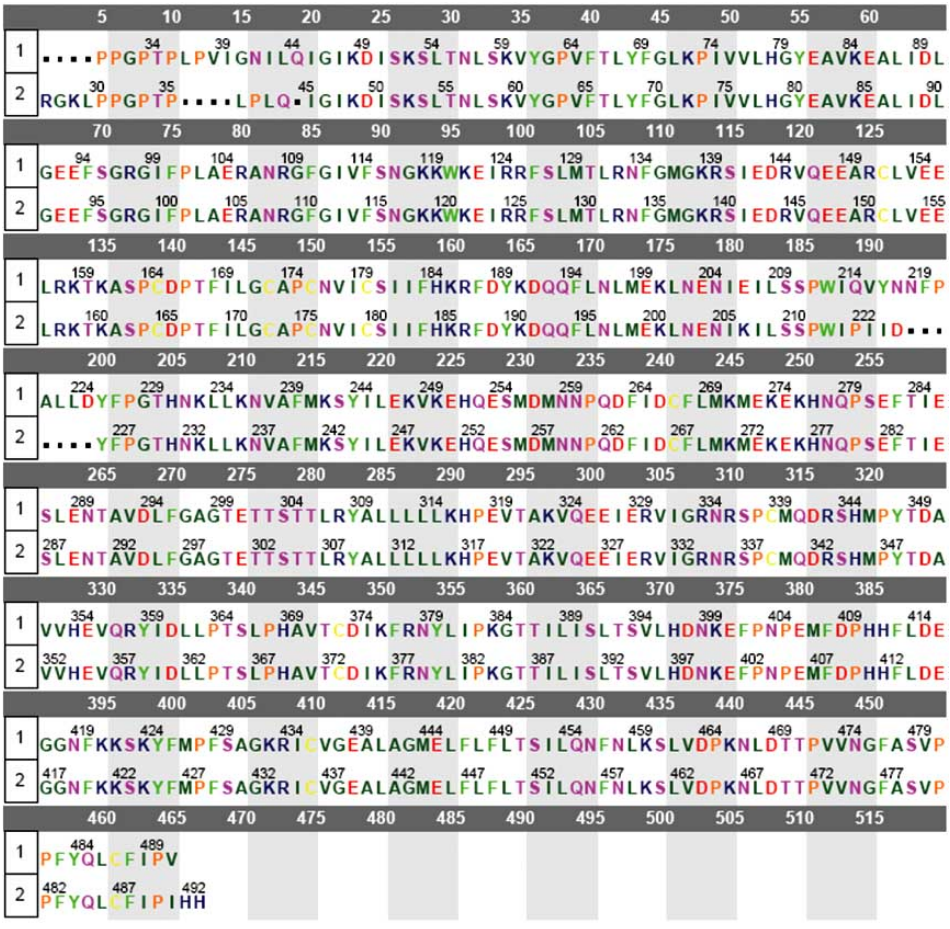

Fig. (1). The sequence alignment between the two crystal structures of CYP2C9 with PDB code 1OG5 (chain-1) and 1R9O (chain-2), where the amino acids are colored according to their function: acidic- red; basic- blue; neutral hydrophilic- pink; aliphatic- dark green; aromatic- light green; thiol containing - yellow; and imino – orange. The two sequences share about 96% sequence identity. (For interpretation of the references to color in this figure legend, the reader is referred to the web version of this paper).

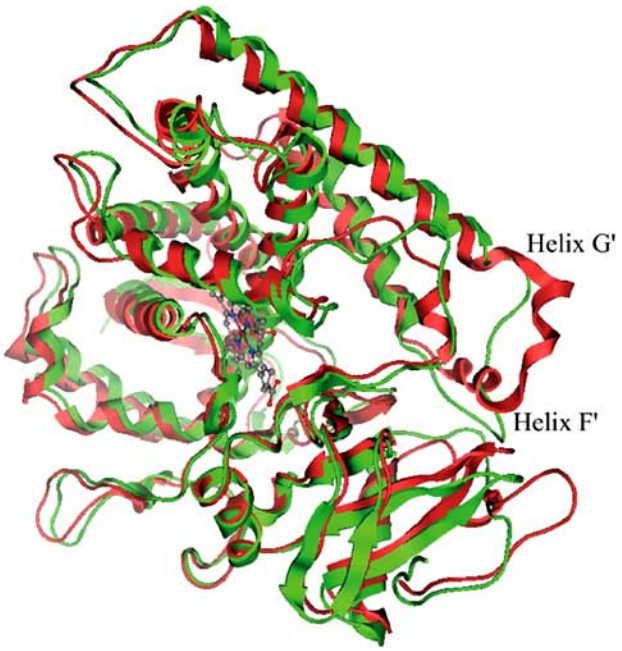

Fig. (2). The two crystal structures of CYP2C9 with PDB code 1R9O (green) and 1OG5 (red). (For interpretation of the references to color in this figure legend, the reader is referred to the web version of this paper).

The three-dimensional structure of CYP2C9 bears the multifaceted and flexible structural feature. To reflect this kind of dynamic features, one of the feasible methods is to utilize molecular dynamics (MD) simulations [79]. The MD simulations can solve the classical equations of motions for a system consisting of target protein and small ligands under specified ensembles. In our case, the energy favorable structures derived by the aforementioned docking experiments were further studied with the molecular dynamics (MD) triggered by breaking hydrogen bonds and making events of the ligand and receptor interactions using GROMACS 3.3.1 package. The results thus obtained would provide further information of the conformational searching in space. The topology files and charges for ligands were generated by the online software RPODRG. At the beginning, all the molecules were inserted into the explicit SPC water of 0.9 nm from the protein surface. To neutralize the system charges, several sodium ions were added to replace the equal numbers of SPC water molecules. Subsequently, all the systems were subjected to a steepest descent energy minimization until a tolerance of 100 kJ/mol. All the molecules were equilibrated with protein backbone fixed at 300 K for some time, then relaxed gradually and heated up to 300 K. Finally, 1 ns MD simulations were performed under the normal temperature and pressure with coupling times of 0.1 ps and 1.0 ps, respectively. This would generate a series of conformations in the important phase space area, providing the configuration and momentum information for each relevant atom, from which the thermodynamic properties of the system can be calculated. Additionally, the electrostatic interactions were computed by the PME algorithm with interpolation order of 4 and a grid spacing of 0.12 nm. The van der Waals interactions were treated by a cut-off of 12 Å. All the simulations were employed with a time step of 2 fs, and coordinates were saved every 1 ps.

The similar methods have been used to investigate the binding interaction of alpha 7 nAChR dimmer with GTS-21 [67], CYP2C19 [60], Xylose reductases [77], and for anti-SARS drug screening [19,66]. For comparison, flurbiprofen has been docked to the crystal structure with PDB code 1R9O, and then optimized by MD simulations. The RMSD between the computational results and crystal data is 0.003.

RESULTS AND DISCUSSIONS

By now, there are two crystal structures releasing in the Protein Data Bank (PDB), namely 1R9O in 2004 [80] and 1OG5 in 2003 [81], respectively. Although having the same sequence (a sequence alignment were performed between the two crystal structures, as shown in Fig. (**1**)), there are some differences between the two crystal structures. It reported that the 1R9O structure of the flurbiprofen complex of 2C9dH corresponds closely to the 1OG5 structure in many regions with a root mean square deviation of 0.74Å, as shown in Fig. (**2**) [80]. In addition, compared with 1OG5, helices F′ and G′ are not evident in 1R9O, which exhibits a more extended conformation of the region between helices F and G, and a longer helix A in 1OG5. As being not far away

Table 1. The Detailed Descriptions of the Five Ligands: Fluoxetine, Ibuprofen, Naproxen, Suprofen, and Mefenamic Acid

Name	Formula	Chemical Name
Fluoxetine	$C_{17}H_{18}F_3NO$	N-methyl-3-phenyl-3-[4-(trifluoromethyl)phenoxy]-propan-1-amine
Ibuprofen	$C_{13}H_{18}O_2$	2-[4-(2-methylpropyl)phenyl] propanoic acid
Diclofenac	$C_{14}H_{11}Cl_2NO_2$	2-[2-[(2,6-dichlorophenyl)amino]phenyl]acetic acid
Suprofen	$C_{14}H_{12}O_3S$	2-(4-thiophen-2-ylcarbonylphenyl) propanoic acid
Mefenamic acid	$C_{15}H_{15}NO_2$	2-[(2,3-dimethylphenyl)amino]benzoic acid

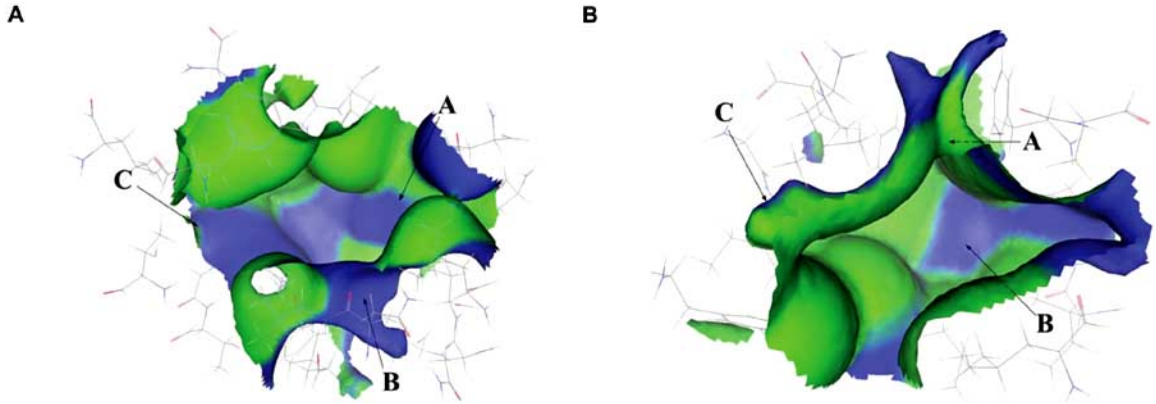

Fig. (3). The binding pocket for (**A**) 1R9O and (**B**) 1OG5. (For interpretation of the references to color in this figure legend, the reader is referred to the web version of this paper).

from the binding site of CYP2C9, these aforementioned differences may cause quite different interactions of CYP2C9 with drugs.

In studying the receptor-ligand binding mechanism, it is very useful to introduce the concept of binding pocket. According to Chou *et al*. [82], the constituents of the binding pocket of a protein receptor to a ligand are defined by those residues that have at least one heavy atom (i.e., an atom other than hydrogen) with a distance $\leq$ 5 Å from a heavy atom of the ligand. Such a criterion was originally used to define the binding pocket of ATP in the Cdk5-Nck5a* complex [82] that has later proved quite useful in identifying functional domains and stimulating the relevant truncation experiments [83]. The similar approach has also been used to define the binding pockets of other receptor-ligand interactions [10,19,60,65,84-86].

As shown in Fig. (**3A**), the binding pocket of 1R9O thus defined assumes bar-shape. There are three regions in the binding pocket of 1R9O, which are considered to be significant for the interactions of CYP2C9 with substrates, as described in Fig. (**3A**). Region **A** and **B** are identity regions, which are in charge of recognizing the corresponding metabolites. Region **C** is oxidation sites, where metabolites may be oxidated by CYP2C9 with heams. As shown in Table **3**, the framework of the binding pocket is constituted by Arg108, Val113, Phe114, Leu201, Asn204, Ile205, Leu208, Val237, Met240, Val292, Asp293, Gly296, Ala297, Thr301, Leu362, Leu366 and Phe476. Among the 17 framework residues, Arg108 and Asn204, which site in the region **A** and **B**, respectively, are more important for having hydrogen bond interactions with all the five drugs. Maybe they play a central role for recognizing and fix metabolites.

In 1OG5, the binding pocket is cross-shape (Fig. **3B**). It extends up with Phe114 and Phe476 lying on the opposite side. Phe476, which showed conformational mobility in the substrate free structure, always forms a π-π stacking interaction with ligand which has a phenyl group as a side chain. The same as 1R9O, the binding pocket of 1OG5 contains three important regions, namely π-π stacking site (region **A**), identify site (region **B**) and oxidation site (region **C**), respectively, as described in Fig. (**3B**). Also, the residues in forming the binding pocket are shown in Table **2**. It is found that Arg97, Gly98, Ile99, Phe100, Pro101, Leu102, Ala103, Val113, Phe114, Leu208, Ile213, Gln214, Asn217, Leu366, Pro367, and Phe476 are significant in forming the framework of the bonding pocket [81]. Also, Asn217 has hydrogen bond interactions with all the five ligands. So, it is found that Asn217 is significant for identifying drugs. In addition, due to the π-π stacking interaction with Phe476, the binding energies of drugs with 1OG5 is much better than 1R9O. Shown in Fig. (**4**) are the binding pockets of 1R9O for (**A**) Fluoxetine, (**B**) Ibuprofen, (**C**) Diclofenac, (**D**) Suprofen, and (**E**) Mefenamic acid, where the lipophilic and hydrophilic

Table 2. List of the Interaction Energies (kcal/mol) Obtained by Docking Fluoxetine, Ibuprofen, Naproxen, and Suprofen to the Two Crystal Structures of CYP2C9 (PDB code 1R9O and 1OG5), Respectively

	E_Intermol		E_Torsional		E_Binding	
Ligands	**1R9O**	**1OG5**	**1R9O**	**1OG5**	**1R9O**	**1OG5**
Fluoxetine	-7.37	-8.69	1.87	1.87	-5.50	-6.99
Ibuprofen	-7.91	-8.84	1.25	1.25	-6.67	-7.60
Diclofenac	-9.17	-9.17	1.25	1.25	-7.93	-7.92
Suprofen	-8.02	-8.90	1.25	1.25	-6.67	-7.65
Mefenamic acid	-8.90	-8.99	0.93	0.93	-7.97	-8.05

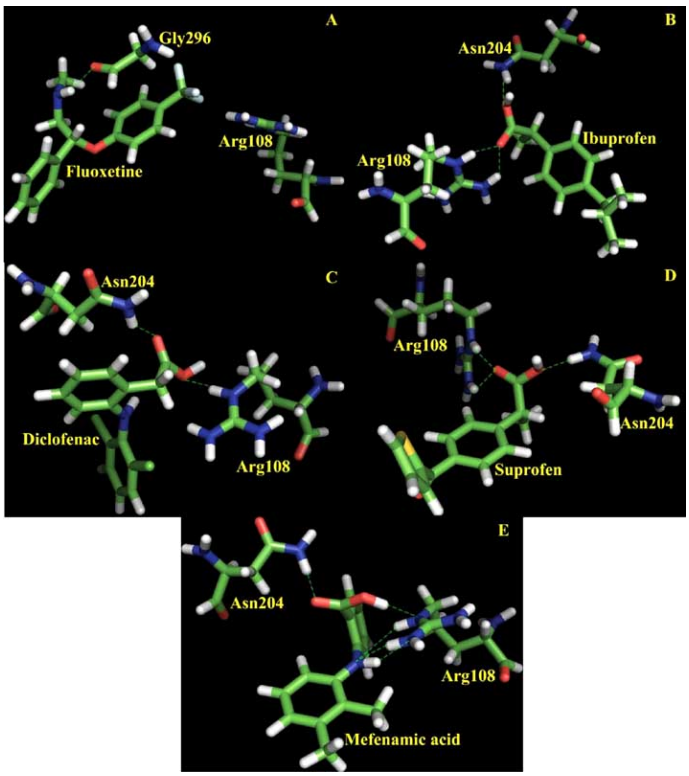

Fig. (4). Illustrations showing the molecular surface of the binding pockets (or cavities) of 1R9O for (**A**) Fluoxetine, (**B**) Ibuprofen, (**C**) Diclofenac, (**D**) Suprofen, and (**E**) Mefenamic acid, where the green dotted lines represent the hydrogen bonds. (For interpretation of the references to color in this figure legend, the reader is referred to the web version of this paper).

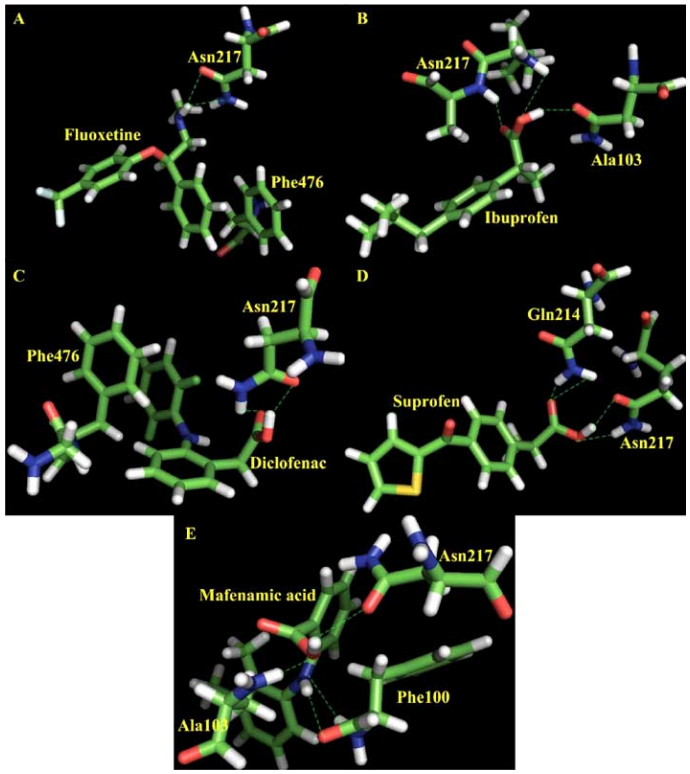

Fig. (5). Illustrations showing the molecular surface of the binding pocket (or cavity) of 1OG5 for (**A**) Fluoxetine, (**B**) Ibuprofen, (**C**) Diclofenac, (**D**) Suprofen, and (**E**) Mefenamic acid, where the green dotted lines represent the hydrogen bonds. (For interpretation of the references to color in this figure legend, the reader is referred to the web version of this paper).

Table 4. Residues in Forming the Binding Pockets of the Crystal Structure of CYP2C9 (PDB Code 1OG5) for the Four Ligands

Ligands	Binding Pocket Residues[a]					
Fluoxetine	Arg97	Gly98	Ile99	Phe100	Pro101	Leu102
	Ala103	Val113	Phe114	Leu208	Ile213	Gln214
	Asn217	Thr364	Ser365	Leu366	Pro367	Leu388
	Phe476					
Ibuprofen	Arg97	Gly98	Ile99	Phe100	Pro101	**Leu102**
	Ala103	Glu104	Val113	Phe114	Leu208	Ile213
	Gln214	**Asn217**	Leu366	Pro367	Phe476	
Diclofenac	Phe100	Pro101	Ala103	Leu208	Ser209	Ser210
	Ile213	Gln214	**Asn217**	Leu362	Thr364	Ser365
	Leu366	Pro367	Leu388	Asn474	Gly475	Phe476
	Ala477					
Suprofen	Arg97	Gly98	Ile99	Phe100	Leu102	Ala103
	Val113	Phe114	Leu208	Ile213	**Gln214**	**Asn217**
	Leu366	Pro367	Gly475	Phe476		
Mefenamic acid	Arg97	Gly98	Ile99	**Phe100**	Pro101	Leu102
	Ala103	Glu104	Val113	Phe114	Leu208	Ile213
	Gln214	**Asn217**	Leu366	Pro367	Phe476	

[a] Residues with bold-face type mean that they have hydrogen bonding interaction with the ligand.

surfaces are colored in green and blue, respectively. Shown in Fig. (**5**) are the binding pocket of 1OG5 for (**A**) Fluoxetine, (**B**) Ibuprofen, (**C**) Diclofenac, (**D**) Suprofen, and (**E**) Mefenamic acid, where the lipophilic and hydrophilic surfaces are colored in green and blue, respectively.

CONCLUSIONS

In order to investigate the interactions of CYP2C9 with diverse drugs, five different kinds of drugs have been docked to the crystal structure of CYP2C9 with PDB code 1OG5 and 1R9O, respectively. It is interested to find that the two binding pocket are quite different. Compared with the bar-shape binding pocket of 1R9O, the binding pocket of 1OG5 is cross-shape, which is more suitable for the interactions with drugs. In addition, Arg108 and Asn204 are found to be the key residues. They may identify the corresponding metabolites by hydrogen bond interactions. All the findings mentioned above will be very useful for conducting mutagenesis studies for finding desired drugs or proper treatments according to the characteristics of an individual patient to improve efficacy and reduce the number and adverse drug reactions.

ACKNOWLEDGEMENTS

This work was supported by the grants from the national 863 Bioinformatics Projects under the contract No. 2007AA02Z333, the national 973 program under the contract No. 2005CB724303 and the Chinese National Science Foundation under the Contract No.20773085 and 30870476, as well as the Major Chinese National Funding of New Drug Discovery for the Integrated Platform and the Virtual Laboratory for Computational Chemistry of CNIC, and the Supercomputing Center of CNIC, Chinese Academy of Sciences.

REFERENCES

[1] Pachabhai, T. S.; Noronha, S. F.; Davis, S.; Shinde, V. M.; Kshirsagar, N. A.; Gogtay, N. J. Evaluation of the activity of CYP2C19 in Gujrati and Marwadi subjects living in Mumbai (Bombay). *BMC Clin. Pharmacol.*, **2006**, *6*, 8.

[2] Gonzalez, F. J.; Skoda, R. C.; Kimura, S.; Umeno, M.; Zanger, U. M.; Nebert, D. W.; Belboin, H. V.; Hardwick, J. P.; Meyer, U. A. Characterization of the common genetic defect in humans deficient in debrisoquine metabolism. *Nature*, **1988**, *331*, 442-446.

[3] Anzenbacher, P.; Anzenbacherova, E. Cytochromes P450 and metabolism of xenobiotics. *Cell Mol. Life Sci.*, **2001**, *58*, 737-747.

[4] Haines, D. C.; Tomchick, D. R.; Machius, M.; Peterson, J. A. Pivotal role of water in the mechanism of P450BM-3. *Biochemistry*, **2001**, *40*, 13456-13465.

[5] Eiselt, R.; Domanski, T. L.; Zibat, A.; Mueller, R.; Presecan-Siedel, E.; Hustert, E.; Zanger, U. M.; Brockmoller, J.; Klenk, H. P.; Meyer, U. A.; Khan, K. K.; He, Y. A.; Halpert, J. R.; Wojnowski, L. Identification and functional characterization of eight CYP3A4 protein variants. *Pharmacogenetics*, **2001**, *11*, 447-458.

[6] Kumana, C. R.; Lauder, I. J.; Chan, M.; Ko, W.; Lin, H. J. Differences in diazepam pharmacokinetics in Chinese and white Caucasians-relation to body lipid stores. *Eur. J. Clin. Pharmacol.*, **1987**, *32*, 211-215.

[7] Lee, C. R.; Goldstein, J. A.; Pieper, J. A. Cytochrome P450 2C9 polymorphisms: a comprehensive review of the *in-vitro* and human data. *Pharmacogenetics*, **2002**, *12*, 251-263.

[8] Chou, K. C. Review: Structural bioinformatics and its impact to biomedical science. *Curr. Med. Chem.*, **2004**, *11*, 2105-2134.

[9] Chou, K. C. Modeling extracellular domains of GABA-A receptors: subtypes 1, 2, 3 and 5. *Biochem. Biophys. Res. Commun.*, **2004**, *316*, 636-642.

[10] Chou, K. C.; Wei, D. Q.; Zhong, W. Z. Binding mechanism of coronavirus main proteinase with ligands and its implication to drug design against SARS. *Biochem. Biophys. Res. Commun.*, **2003**, *308*, 148-151. (Erratum: ibid., **2003**, *310*, 675)

[11] Li, Y.; Wei, D. Q.; Gao, W. N.; Gao, H.; Liu, B. N.; Huang, C. J.; Xu, W. R.; Liu, D. K.; Chen, H. F.; Chou, K. C. Computational approach to drug design for oxazolidinones as antibacterial agents. *Med. Chem.*, **2007**, *3*, 576-582.

[12] Wang, J. F.; Wei, D. Q.; Chen, C.; Li, Y. X.; Chou, K. C. Molecular modeling of two CYP2C19 SNPs and its implications for personalized drug design. *Protein Pept. Lett.*, **2008**, *15*, 27-32.

[13] Zhang, R.; Wei, D. Q.; Du, Q. S.; Chou, K. C. Molecular modeling studies of peptide drug candidates against SARS. *Med. Chem.*, **2006**, *2*, 309-314.

[14] Gao, W. N.; Wei, D. Q.; Li, Y.; Gao, H.; Xu, W. R.; Li, A. X.; Chou, K. C. Agaritine and its derivatives are potential inhibitors against HIV proteases. *Med. Chem.*, **2007**, *3*, 331-336.

[15] Zheng, H.; Wei, D. Q.; Zhang, R.; Wang, C.; Wei, H.; Chou, K. C. Screening for new agonists against Alzheimer's disease. *Med. Chem.*, **2007**, *3*, 488-493.

[16] Chou, K. C.; Nemethy, G.; Scheraga, H. A. Energetic approach to packing of alpha-helices: 2. General treatment of nonequivalent and monregular helices. *J. Am. Chem. Soc.*, **1984**, *106*, 3161-3170.

[17] Chou, K. C.; Maggiora, G. M.; Nemethy, G.; Scheraga, H. A. Energetic of the structure of the four-alpha-helix boundle in proteins. *Proc. Natl. Acad. Sci. USA*, **1988**, *85*, 4295-4299.

[18] Sirois, S.; Wei, D. Q.; Du, Q. S.; Chou, K. C. Virtual screening for SARS-CoV protease based on KZ7088 pharmacophore points. *J. Chem. Inf. Comput. Sci.*, **2004**, *44*, 1111-1122.

[19] Chou, K. C.; Wei, D. Q.; Du, Q. S.; Sirois, S.; Zhong, W. Z. Review: Progress in computational approach to drug development against SARS. *Curr. Med. Chem.*, **2006**, *13*, 3263-3270.

[20] Chou, K. C. Energy-optimized structure of antifreeze protein and its binding mechanism. *J. Mol. Biol.*, **1992**, *223*, 509-517.

[21] Zhou, G. P.; Deng, M. H. Anextension of Chou's graphical rules for deriving enzyme kinetic equations to system involving parallel reaction pathways. *Biochem. J.*, **1984**, *222*, 169-176.

[22] Myers, D.; Palmer, G. Microcomputer tools for steady-state enzyme kinetics. *Bioinformatics*, **1985**, *1*, 105-110.

[23] Chou, K. C. Graphical rules in steady and non-steady enzyme kinetics. *J. Biol. Chem.*, **1989**, *264*, 12074-12079.

[24] Chou, K. C. Review: Applications of graph theory to enzyme kinetics and protein folding kinetics. Steady and non-steady state systems. *Biophys. Chem.*, **1990**, *35*, 1-24.

[25] Althaus, I. W.; Chou, J. J.; Gonzales, A. J.; Diebel, M. R.; Chou, K. C. Kezdy, F. J.; Romero, D. L.; Aristoff, P. A.; Tarpley, W. G.; Reusser, F. Steady-state kinetic studies with the non-nucleoside HIV-1 reverse transcriptase inhibitor U-87201E. *J. Biol. Chem.*, **1993**, *268*, 6119-6124.

[26] Chou, K. C.; Zhang, C. T. Diagrammatization of codon usage in 339 HIV proteins and its biological implication. *AIDS Res. Hum. Retroviruses*, **1992**, *8*, 1967-1976.

[27] Althaus, I. W.; Gonzales, A. J.; Chou, J. J.; Diebel, M. R.; Chou, K. C.; Kezdy, F. J.; Romero, D. L.; Aristoff, P. A.; Tarpley, W. G.; Reusser, F. The quinoline U-78036 is a potent inhibitor of HIV-1 reverse transcriptase. *J. Biol. Chem.*, **1993**, *268*, 14875-14880.

[28] Althaus, I. W.; Chou, J. J.; Gonzales, A. J.; Diebel, M. R.; Chou, K. C.; Kezdy, F. J.; Romero, D. L.; Aristoff, P. A.; Tarpley, W. G.; Reusser, F. Kinetic studies with the nonnucleoside HIV-1 reverse transcriptase inhibitor U-88204E. *Biochemistry*, **1993**, *32*, 6548-6554.

[29] Chou, K. C.; Kezdy, F. J.; Reusser, F. Review: Steady-state inhibition kinetics of processive nucleic acid polymerases and nucleases. *Anal. Biochem.*, **1994**, *221*, 217-230.

[30] Andraos, J. Kinetic plasticity and the determination of product ratios for kinetic schemes leading to multiple products without rate laws: new methods based on directed graphs. *Can. J. Chem.*, **2008**, *86*, 342-357.

[31] Wang, M.; Yao, J. S.; Huang, Z. D.; Xu, Z. J.; Liu, G. P.; Zhao, H. Y.; Wang, X. Y.; Wang, J.; Zhu, Y. S.; Chou, K. C. A new nucleotide-composition based fingerprint of SARS-CoV with visualization analysis. *Med. Chem.*, **2005**, *1*, 39-47.

[32] Xiao, X.; Shao, S.; Ding, Y.; Huang, Z.; Chen, X.; Chou, K. C. An application of gene comparative image for predicting the effect on replication ratio by HBV virus gene missense mutation. *J. Theor. Biol.*, **2005**, *235*, 555-565.

[33] Xiao, X.; Shao, S. H.; Chou, K. C. A probability cellular automation model for hepatitis B viral infections. *Biochem. Biophys. Res. Commun.*, **2006**, *342*, 605-610.

[34] Chou, K. C. Review: Low-frequency collective motion in biomacromolecules and its bioligcal functions. *Biophys. Chem.*, **1988**, *30*, 3-48.

[35] Chou, K. C. Low-frequency resonance and cooperativity of hemoglobm. *Trends Biochem. Sci.*, **1989**, *14*, 212.

[36] Chou, K. C.; Mao, B. Collective motion in DNA and its role in drug interactions. *Biopolymers*, **1988**, *27*, 1795-1815.

[37] Prado-Prado, F. J.; Gonzalez-Diaz, H.; de la Vega, O. M.; Ubeira, F. M.; Chou, K. C. Unified QSAR model for input-coded prediction, structural back-projection, and complex networks clustering of antrprotozoal compounds. *Bioorg. Med. Chem.*, **2008**, *16*, 5871-5880.

[38] Dea-Ayuela, M A.; Perez-Castillo, Y.; Meneses-Marcel, A.; Ubeira, F. M.; Bolas-Fernandez, F.; Chou, K. C.; Gonzalez-Diaz, H. HP-lattice QSAR for dynein proteins: experimental proteomics (2D-electrophoresis, mass spectrometry) and theoretic study of a Leishmania infantum sequence. *Bioorg. Med. Chem.*, **2008**, *16*, 7770-7776.

[39] Du, Q. S.; Mezey, P. G.; Chou, K. C. Heuristic molecular lipophilicity potential (HMLP): a 2D-QSAR study to LADH of molecular family pyrazole and derivatives. *J. Comput. Chem.*, **2005**, *26*, 461-470.

[40] Du, Q. S.; Huang, R. B.; Wei, Y. T.; Du, L. Q.; Chou, K. C. Multiple filed three dimensional quantitative structure-activity relationship (MF-3D-QSAR). *J. Comput. Chem.*, **2008**, *29*, 211-219.

[41] Du, Q. S.; Huang, R. B.; Chou, K. C. Review: Recent advances in QSAR and their applications in predicting the activities of chemical molecules, peptides and proteins for drug design. *Curr. Protein Pept. Sci.*, **2008**, *9*, 248-259.

[42] Du, Q. S.; Huang, R. B.; Wei, Y. T.; Pang, Z. W.; Du, L. Q.; Chou, K. C. Fragment-based quantitative structure-activity relationship (FB-QSAR) for fragment-based drug design. *J. Comput. Chem.*, **2008**, *30*, 295-304.

[43] Chou, K. C.; Shen, H. B. Cell-PLoc: A package of web-servers for predicting subcellular localization of proteins in various organisms. *Nat. Protoc.*, **2008**, *3*, 153-162.

[44] Chou, K. C.; Shen, H. B. Review: Recent progresses in protein subcellular location prediction. *Anal. Biochem.*, **2007**, *370*, 1-16.

[45] Jiang, X.; Wei, R.; Zhang, T. L.; Gu, Q. Using the concept of Chou's pseudo amino acid composition to predict apoptosis proteins subcellular location: an approach by approximate entropy. *Protein Pept. Lett.*, *2008*, *15*, 392-396.

[46] Li, F. M.; Li, Q. Z. Predicting protein subcellular location using Chou's pseudo amino acid composition and improved hybrid approach. *Protein Pept. Lett.*, **2008**, *15*, 612-616.

[47] Lin, H.; Ding, H.; Guo, F. B.; Zhang, A. Y.; Huang, J. Predicting subcellular localization of mycobacterial proteins by using Chou's pseudo amino acid composition. *Protein Pept. Lett.*, **2008**, *15*, 739-744.

[48] Ding, Y. S.; Zhang, T. L. Using Chou's pseudo amino acid composition to predict subcellular localization of apoptosis proteins: an approach with immune genetic algorithm-based ensemble classifier. *Pattern Recognit. Lett.*, **2008**, *29*, 1887-1892.

[49] Chou, K. C.; Shen, H. B. MemType-2L: A web server for predicting membrane proteins and their types by incorporating evolution information through Pse-PSSM. *Biochem. Biophys. Res. Commun.*, **2007**, *360*, 339-345.

[50] Shen, H. B.; Chou, K. C. EzyPred: A top-down approach for predicting enzyme functional classes and subclasses. *Biochem. Biophys. Res. Commun.*, **2007**, *364*, 53-59.

[51] Chou, K. C. Prediction of G-protein-coupled receptor classes. *J. Proteome Res.*, **2005**, *4*, 1413-1418.

[52] Xiao, X.; Wang, P.; Chou, K. C. GPCR-CA: A cellular automaton image approach for prediction G-protein-coupled receptor functional classes. *J. Comput. Chem.*, **2008**, DOI 10.1002/jcc.21163.

[53] Chou, K. C.; Shen, H. B. ProtIdent: A web server for identifying proteases and their types by fusing functional domain and sequential evolution information. *Biochem. Biopohys. Res. Commun.*, **2008**, *376*, 321-325.

[54] Shen, H. B.; Chou, K. C. Identification of proteases and their types. *Anal. Biochem.*, **2009**, *385*, 153-160.

[55] Chou, K. C. A vectorized sequence-coupling model for predicting HIV protease cleavage sites in proteins. *J. Biol. Chem.*, **1993**, *268*, 16938-16948.

[56] Chou, K. C. Review: Prediction of HIV protease cleavage sites in proteins. *Anal. Biochem.*, **1996**, *233*, 1-14.

[57] Shen, H. B.; Chou, K. C. HIVcleave: a web-server for predicting HIV protease cleavage sites in proteins. *Anal. Biochem.*, **2008**, *375*, 388-390.

[58] Chou, K. C.; Shen, H. B. Signal-CF: a subsite-coupled and window-fusing approach for predicting signal peptides. *Biochem. Biophys. Res. Commun.*, **2007**, *357*, 633-640.

[59] Shen, H. B.; Chou, K. C. Sinal-3L: a 3-layer approach for predicting signal peptide. *Biochem. Biophys. Res. Commun.*, **2007**, *363*, 297-303.

[60] Wang, J. F.; Wei, D. Q.; Li, L.; Zheng, S. Y.; Li, Y. X.; Chou, K. C. 3D structure modeling of cytochrome P450 2C19 and its implication for personalized drug design. *Biochem. Biophys. Res. Commun.*, **2007**, *355*, 513-519. (Corrigendum: ibid, 2007, Vol. 357, 330)

[61] Wang, J. F.; Wei, D. Q.; Li, L.; Chou, K. C. Review: Pharmacogenomics and personalized use of drugs. *Curr. Topics Med. Chem.*, **2008**, *8*, 1573-1579.

[62] Wang, J. F.; Zhang, C. C.; Chou, K. C.; Wei, D. Q. Review: Structure of cytochrome P450s and personalized drug. *Curr. Med. Chem.*, **2009**, *16*, 232-244.

[63] Wang, J. F.; Zhang, C. C.; Yan, J. Y.; Chou, K. C.; Wei, D. Q. In *Automation in Genomics and Proteomics: An Engineering Case-Based Approach*, Chapter 11; Benson, R.; Alterovitz, G.; Marco-Ramoni, M.; Wiley: Boston, **2009**.

[64] Li, H.; Poulos, T. L. Conformational dynamics in cytochrome P450-substrate interactions. *Biochimie*, **1996**, *78*, 695-699.

[65] Chou, K. C. In Frontiers in Medicinal Chemistry, Atta-ur-Rahman, Reitz, A. B., Ed.; Bentham Science Publishers: the Netherlands, **2006**, Vol. 3, pp. 455-502.

[66] Wei, D. Q.; Zhang, R.; Du, Q. S.; Gao, W. N.; Li, Y.; Gao, H.; Wang, S. Q.; Zhang, X.; Li, A. X.; Sirois, S.; Chou, K. C. Anti-SARS drug screeing by molecular docking. *Amino Acids*, **2006**, *31*, 73-80.

[67] Wei, D. Q.; Sirois, S.; Du, Q. S.; Arias, H. R.; Chou, K. C. Theortical studies of Alzheimer's disease drug candidate [(2,4-dimethoxy)benzylidene]-anabaseine dihydrochloride (GTS-21) and its derivatives. *Biochem. Biophys. Res. Commun.*, **2005**, *338*, 1059-1064.

[68] Zhou, G. P.; Troy, F. A. 2nd NMR study of the preferred membrane orientation of polyisoprenols (dolichol) and the impact of their complex with polyisoprenyl recognition sequence peptides on membrane structure. *Glycobiology*, **2005**, *15*, 347-359.

[69] Zhou, G. P.; Troy, F. A. NMR studies on how the binding complex of polyisoprenol recognition sequence peptides and polyisoprenols can modulate membrane structure. *Curr. Protein Pept. Sci.*, **2005**, *6*, 399-411.

[70] Wei, H.; Zhang, R.; Wang, C.; Zheng, H.; Chou, K. C.; Wei, D. Q. Molecular insights of SAH enzyme catalysis and their implication for inhibitor design. *J. Theor. Biol.*, **2007**, *244*, 692-702.

[71] Du, Q. S.; Wang, S.; Wei, D. Q.; Sirois, S.; Chou, K. C. Molecular modeling and chemical modification for finding peptide inhibitor against SARS CoV Mpro. *Anal. Biochem.*, **2005**, *337*, 262-270.

[72] Li, L.; Wei, D. Q.; Wang, J. F.; Chou, K. C. Computational studies of the binding mechanism of calmodulm with chrysin. *Biochem. Biophys. Res. Commun.*, **2007**, *358*, 1102-1107.

[73] Guo, X. L.; Li, L.; Wei, D. Q.; Zhu, Y. S.; Chou, K. C. Cleavage mechanism of the H5N1 hemagglutinin by trypsin and furin. *Amino Acids*, **2008**, *35*, 375-382.

[74] Wang, S. Q.; Du, Q. S.; Zhao, K.; Li, A. X.; Wei, D. Q.; Chou, K. C. Virtual screening for finding natural inhibitor against cathepsin-L for SARS therapy. *Amino Acids*, **2007**, *33*, 129-135.

[75] Du, Q. S.; Wang, S. Q.; Jiang, Z. Q.; Gao, W. N.; Li, Y. D.; Wei, D. Q.; Chou, K. C. Application of bioinformatics in search for cleavable peptides of SARS-CoV Mpro and chemical modification of octapeptides. *Med. Chem.*, **2005**, *1*, 209-213.

[76] Du, Q. S.; Sun, H.; Chou, K. C. Inhibitor design for SARS coronavirus main protease based on "distorted key theory". *Med. Chem.*, **2007**, *3*, 1-6.

[77] Wang, J. F.; Wei, D. Q.; Lin, Y.; Wang, Y. H.; Du, H. L.; Li, Y. X.; Chou, K. C. Insights from modeling the 3D structure of NAD(P)H-dependent D-xylose reductase of *Pichia stipitis* and its binding interactions with NAD and NADP. *Biochem. Biophys. Res. Commun.*, **2007**, *359*, 323-329.

[78] Morris, G. M.; Goodsell, D. S.; Halliday, R. S.; Huey, R.; Hart, W. E.; Belew, R. K.; Olson, A. J. Automated docking using a Lamarckian Genetic Algorithm and empirical binding free energy function. *J. Comput. Chem.*, **1998**, *19*, 1639-1662.

[79] Allen, M. P.; Wilson, M. R. Computer simulation of liquid crystals. *J. Comput. Aided Mol. Des.*, **1989**, *3*, 335-353.

[80] Wester, M. R.; Yano, J. K.; Schoch, G. A.; Yang, C.; Griffin, K. J.; Stout, C. D.; Johnson, E. F. The structure of human cytochrome P450 2C9 complexed with flurbiprotein at 2.0-A resolution. *J. Biol. Chem.*, **2004**, *279*, 35630-35637.

[81] Williams, P. A.; Cosme, J.; Ward, A.; Angove, H. C.; Matak-Vinkovic, D.; Jhoti, H. Crystal structure of human cytochrome P450 2C9 with bound warfarin. *Nature*, **2003**, *424*, 464-468.

[82] Chou, K. C.; Watenpaugh, K. D.; Heinrikson, R. L. A model of the complex between cyclin-dependent kinase 5 (Cdk5) and the activation domain of neuronal Cdk5 activation. *Biochem. Biophys. Res. Commun.*, **1999**, *259*, 420-428.

[83] Zhang, J.; Luan, C. H.; Chou, K. C.; Johnson, G. V. W. Identification of the N-terminal functional domain of Cdk5 by molecular truncation and computer modeling. *Proteins.*, **2002**, *48*, 447-453.

[84] Chou, K. C. Insights from modeling the 3D structure of the extracellular domain of alpha 7 nicotinic acetylcholine receptor. *Biochem. Biophys. Res. Commun.*, **2004**, *319*, 433-438.

[85] Wei, D. Q.; Du, Q. S.; Sun, H.; Chou, K. C. Insights from modeling the 3D structure of H5N1 influenza virus neuraminidase and its binding interactions with ligands. *Biochem. Biophys. Res. Commun.*, **2006**, *344*, 1048-1055.

[86] Wang, S. Q.; Du, Q. S.; Chou, K. C. Study of drug resistance of chicken influenza A virus (H5N1) from homology-modeled 3D structures of neuraminidases. *Biochem. Biophys. Res. Commun.*, **2007**, *354*, 634-640.

Received: 20 November, 2008 **Revised: 05 March, 2008** **Accepted: 20 March, 2008**